Asian Journal of Information Technology 5 (11): 1245-1247, 2006
© Medwell Journals, 2006

FEM Analysis of Cage Stress Distribution Part 2: Angular Contact Ball Bearing

A. Dib, M. Benamira and A. Haiahem
Laboratoire de Mécanique Industrielle (LMI), Annaba University, Algeria

Abstract: This study reports on a numerical study of angular contact ball bearing cage. The analysis is based on finite element method. The results show that traction stress is the cause of the failure of the cage. Stress concentration is located in the thin width of the hole of the cage. The traction stress lies around the hole of the cage where the contact between the ball and the cage. The most effect of cage damage is the traction stress in the thin width of the cage.

Key words: Angular contact ball bearing, cage, FEM, stress distribution

INTRODUCTION

Since 1976, a few attempts have been carried out in order to evaluate the internal kinematics[1-3]. In this field, the studies based on computer programs, such as Cybean[4], Shaberth[5] or Adore[6] can be noted. All of these studies do not take into account a deformation of the cage. Recently[7,8], cage instability has been studied as a function of the roller-race and roller cage pocket clearances light-load and high-speed condition. The results indicate that the cage exhibits stable motion for small values of roller-race and roller-cage pocket clearance.

The aim of the current investigation is to provide a better understanding of the stress distribution in angular contact ball bearing cage using Finite Element Method (FEM).

Governing equations: As shown schematically in Fig. 1, the dominant velocity for the roller/cage will be the roller velocity about x axis. It will be assumed the entire hydrodynamic action takes place on the ball surface only. The maximum pressure is obtained by resolving two-dimension Reynolds equation. The global balance of the angular contact ball bearing was not tacking into account. The study is focus in the local interaction between the cage and the ball.

Analysis of this contact involved the solution of two-dimensional Reynolds equation in X and Y direction. Integration the pressure over the contact area gives us the total load.

The assumptions used in the analysis are:

- The surfaces are essentially rigid and circular rand, the spacing between them can be presented by a parabolic approximation.
- A full film lubricant exists between the surfaces.
- The lubricant is Newtonian with a constant viscosity.

The Reynolds equation is written as

$$\frac{\partial}{\partial x}\left(h^3\frac{\partial p}{\partial x}\right)+\frac{\partial}{\partial z}\left(h^3\frac{\partial p}{\partial z}\right)=6\mu(u_1-u_2)\frac{\partial h}{\partial x}+12V_2 \quad (1)$$

with

$$\frac{V_2}{u_2}=tg(\alpha)=\frac{\partial h}{\partial x} \quad (2)$$

and

$$u_2=R_x\,\omega \quad (3)$$

In our study $u_1 = 0$;

Substitution (2) and (3) in (1), Reynolds equation becomes:

$$\frac{\partial}{\partial x}\left(h^3\frac{\partial p}{\partial x}\right)+\frac{\partial}{\partial z}\left(h^3\frac{\partial p}{\partial z}\right)=6\mu\,U\frac{\partial h}{\partial x_2} \quad (4)$$

with

$$U=R_x\,\omega \quad (5)$$

The boundary conditions are:
In x direction:

$$\begin{cases} p=0 \text{ and } \dfrac{\partial p}{\partial x}=0 \text{ at inlet zone} \\ p=0 \text{ at outlet zone} \end{cases} \quad (6)$$

Corresponding Author: A. Dib, Laboratoire de Mécanique Industrielle (LMI), Annaba University, Algeria

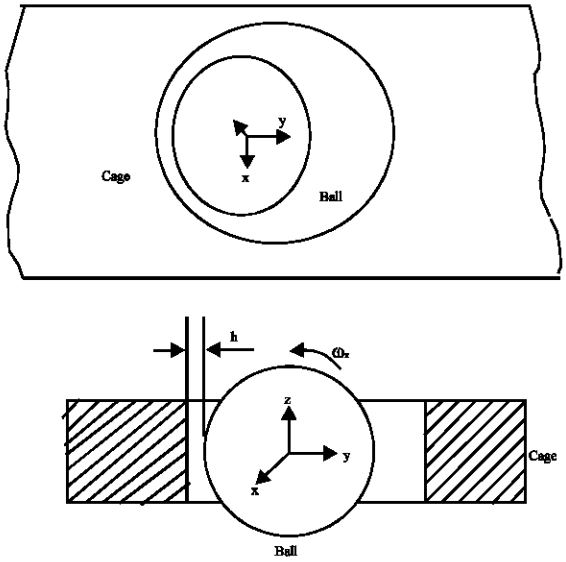

Fig. 1: Hydrodynamic interaction between the cage and the ball

In y direction:

$$\begin{cases} p = 0 \quad \text{and} \quad \dfrac{\partial p}{\partial z} = 0 \text{ at inlet zone} \\ P = 0 \text{ at } \dfrac{\partial p}{\partial z} = 0 \text{ at outlet zone} \end{cases} \tag{7}$$

Kapista[9] has given the following solution

$$p(x \cdot z) = \frac{-6\mu U}{3 + \dfrac{2}{R}} \cdot \frac{x}{h^2} \quad \text{with} \quad R = \frac{R_z}{R_x} \tag{8}$$

Integrating the pressure

$$W = 2\int_{0}^{\infty}\int_{-\infty}^{0} p \, dx \, dz \tag{9}$$

Substitution (8) in (9)

$$W = -\frac{12\mu U}{3 + \dfrac{2}{R}} \int_{0}^{+\infty} \left[\int_{-\infty}^{0} \frac{x \, dx}{\left(h_0 + \dfrac{x^2}{2R_x} + \dfrac{z^2}{2R_z} \right)^2} \right] dz \tag{10}$$

Finally, the total load supported between the contact is:

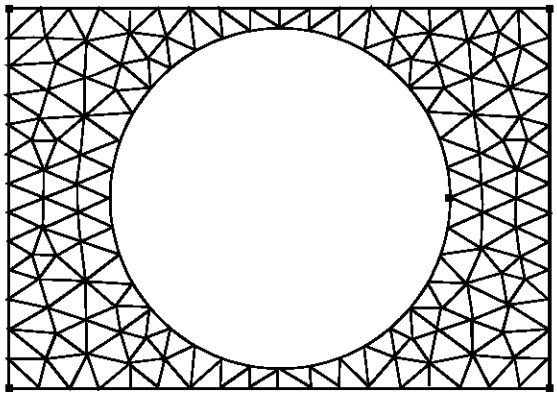

Fig. 2: Mailed cage

Fig. 3: Stress distribution in the whole cage

$$W = \frac{6\mu R_x \pi \sqrt{2R_x}\, U}{3 + \dfrac{2}{R}} \bullet h_0^{-\frac{1}{2}} \tag{11}$$

Operating conditions: The material of the cage is the bronze. The ball material is 10Cr6. the dimension of the cage and the load applied are shown in Table 1.

RESULTS AND DISCUSSION

The area is divided into 240 elements and 169 nodes as shown in Fig. 2. The code used in this study is RDM6. The variation of the traction stress in direction of the traction force is shown in Fig. 3. It is obvious that the stress rises in the thin width of the cage. The stress traction σ_{xx} exceed the value of young modulus, causing a plastic deformation in this area. The deformation of the cage Fig. 4 confirms that thin width of cage is the most deformed area. The compressive stress is located far from the interaction between the cage and the ball. According to Fig. 3, the thin width of the cage is subjected to a

Table 1: Operating conditions of the cage

Dimensions and loads	Values
Diameter of the ball, D	12 mm
Diameter of the cage hole, DC	12.6 mm
Width of the cage, L_c	14 mm
Axial load, Q_a	8900 N
Radial load, Qr	5500 N
Lubricant viscosity, μ	0.04 N s m^{-2}
Angular ball vilocty, $\dot{u}_c$	400 rad s^{-1}
Contact angle, α	40°

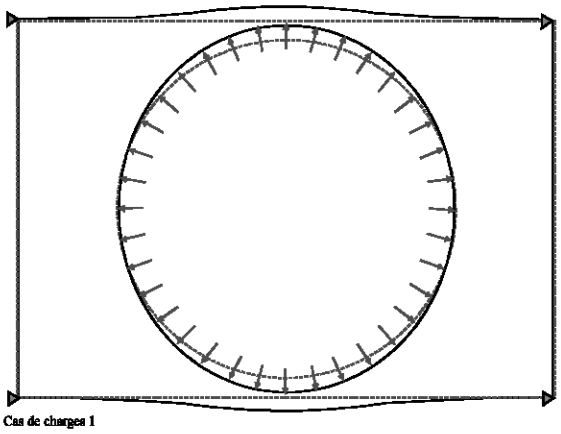

Fig. 4: Deformed cage

traction stress in y direction. The value of this stress is higher than elastic modulus, so this area can be deformed plastically.

CONCLUSION

The results show that traction stress is the cause of the failure of the cage. Stress concentration is located in thin width of the hole of the cage. The compressive stress lies in the Y direction but does not cause damage. The most effect of cage damage is the traction stress in the thin width the cage.

REFERENCES

1. Bonnes, R.J., 1970. The effect of oil supply on cage and roller motion in lubricated roller bearing, ASME J. Lubrication Tech., 69-LUB 8-7, pp: 39-53.
2. Poplawski, J.V., 1972. Slip and cage forces in a high-speed roller bearing, ASME J. Lubrication Tech., 71-LUB-17, pp: 143-152.
3. Berth, D. and L. Flamand, 1982. Skidding in Roller Bearings, Effect of Lubricant, Proc. AGARD Symp. Ottawa, pp: 323.
4. Kleckner, R.J., J. Prvics and V. Castelli, 1980. High speed cylindrical rolling element bearing analysis CYBEAN-analatic formulation, ASME J. Lubrication Tech., 102: 380-390.
5. Hadden, G.B., R.J. Kleckner, M.A. Regan and L. Sheynin, 1981. Research repport-user'smanual for computer program AT81Y003 Shaberth. Steady state and transient thermal analysis of a haft bearing system including ball, cylindrical and tapered roller bearing, NASA, Washington, DC, NASA CR, 165365.
6. Gupta, P.K., 1984. Advanced dynamics of rolling elements, Springer-Verlag, New-York, pp: 295.
7. Niranjan, G., R.W. Carl and S. Farshid, 2004. Cage instabilities in cylindrical roller bearings ASME J. Tribology, 126: 681-689.
8. Neng Tung, L. and L. Jen Fin, 2002. Ball bearing skidding under radial and axial loads, Mechanism and Machine Theory, 37: 91-113.
9. Kapitsa, H.S., 1955. Lubrication of rollers and spheres, Zhur. Tekh. Fiz, 25: 747-762.